Differential Scanning Calorimetry Study of Glass Transition in Frozen Starch Gels

KANITHA TANANUWONG AND DAVID S. REID*

Department of Food Science and Technology, University of California, Davis, 1 Shields Avenue, Davis, California 95616

The effects of initial water content, maximum heating temperature, amylopectin crystallinity type, and annealing on the glass transition of starch gels were studied by differential scanning calorimetry (DSC). The glass transition temperatures of the frozen gels measured as the onset ($T_{g,onset}$*) or midpoint temperature ($T_{g,midpoint}$*), heat capacity change during the glass transition (ΔC_p), unfrozen water of starch gels, and additional unfrozen water (AUW) arising from gelatinization were reported. The results show that $T_{g,onset}$* and $T_{g,midpoint}$* of the partially gelatinized gels are independent of the initial water content, while both of the T_g* values of the fully gelatinized gel increase as the initial water content increases. These observations might result from the difference in the level of structural disruption associated with different heating conditions, resulting in different gel structures as well as different concentrations of the sub-T_g unfrozen matrix. The amylopectin crystallinity type does not greatly affect $T_{g,onset}$* and $T_{g,midpoint}$* of the gels. Annealing at a temperature near $T_{g,onset}$* increases both $T_{g,onset}$* and $T_{g,midpoint}$* of the gels, possibly due to an increase in the extent of the freeze concentration as evidenced by a decrease in AUW. Annealing results in an increase in the ΔC_p value of the gels, presumably due to structural relaxation. A devitrification exotherm may be related to AUW. The annealing process decreases AUW, thus also decreasing the size of the exotherm.

KEYWORDS: Starch; glass transition; differential scanning calorimetry; gelatinization; annealing

INTRODUCTION

The processing of starch-based foods usually involves heating starch in the presence of water to a temperature above the gelatinization temperature, causing disruption of the starch granule structure. During gelatinization, the semicrystalline polymer structure in native granular starches is gradually transformed into an amorphous state, which is metastable and subject to time-dependent physical change (*1*, *2*). An important example is recrystallization of amylopectin in starch gels, which greatly affects the textural properties of starch-based foods (*2*). Sufficient cooling of an amorphous polymer can induce a phase transformation of the rubbery amorphous matrix to a glassy, solid matrix. This transition, denoted as a glass transition, is evidenced by both a large increase in the viscosity and an immobilization of the polymer chains (*1*). In general, the glass transition largely relates to the changes in quality and storage stability of food products (*1*, *3*, *4*). Depending on the storage temperature and the composition of the system, the amorphous phase can exist in the glassy state, rigid and stable, or become rubbery and prone to physical and chemical changes (*4*).

For a high moisture system, the glass transition temperature of a homogeneous amorphous matrix, $T_{g,C}$ (given the initial solute concentration of C_c) is predicted to be below the freezing

temperature of the system, $T_{m,C}$ (**Figure 1**). During cooling, ice crystallization can occur before the system reaches $T_{g,C}$. The system is then separated into an ice phase and an unfrozen phase. As the temperature lowers, more ice is formed, with a resulting increase in the concentration of the unfrozen matrix. At a sufficiently low temperature, this freeze-concentrated unfrozen phase solidifies into the glassy state and ice formation ceases because of kinetic restrictions (*5*, *6*). In a system in which the maximum amount of ice is allowed to form, the glass transition of this maximally freeze-concentrated phase occurs at T_g', which is independent of the initial solute concentration (*7*). T_g' may be an important parameter for the quality and stability of frozen food systems, as a long-term stability may be anticipated for the product stored at a temperature below T_g' (*4*, *8*). If the maximum amount of ice is not formed in the system, the resulting unfrozen matrix will be more dilute. The glass transition temperature of this partially freeze-concentrated phase, denoted as T_g*, is lower than T_g'. Along the T_g curve, T_g* will fall between $T_{g,C}$ and T_g', depending on the concentration of the unfrozen phase (the shaded gray area in **Figure 1**). The exact value of T_g* will depend on the imposed conditions (*9*).

For low moisture starch systems (13−30% moisture) after heating to over 100 °C, the glass transition temperature (T_g) decreases as the moisture content increases due to the plasticization effect of water. At a moisture content greater than 22%, T_g

* To whom correspondence should be addressed. Tel: +1-530-752-8448. Fax: +1-530-752-4759. E-mail: dsreid@ucdavis.edu.
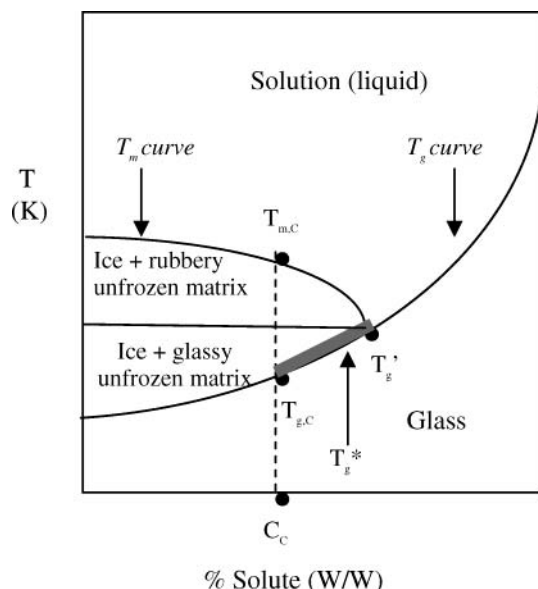
Glass Transition in Frozen Starch Gels

J. Agric. Food Chem., Vol. 52, No. 13, 2004 **4309**

Figure 1. State diagram of the binary aqueous system.

Table 1. Target Temperatures Used in the DSC Temperature Programs in **Figure 2a**

water content (g water/ g dry starch)	target temperatures (°C) related to the gelatinization endotherms							
	waxy corn		normal corn		potato		pea	
	$T_1{}^a$	$T_2{}^b$	T_1	T_2	T_1	T_2	T_1	T_2
1.10	72.5	100.0	72.5	95.0	64.0	95.0	71.5	110.0
1.30	72.5	95.0	72.5	95.0	64.0	90.0	71.5	105.0
1.50	72.5	90.0	72.5	90.0	64.0	90.0	71.5	100.0
1.75	72.5	90.0	72.5	85.0	64.0	85.0	71.5	95.0
2.00	72.5	90.0	72.5	85.0	64.0	80.0	71.5	95.0
2.50	72.5	90.0	72.5	85.0	64.0	80.0	71.5	90.0
3.00	72.5	90.0	72.5	85.0	64.0	80.0	71.5	90.0

a The temperature near the peak temperature of the first endotherm (G endotherm). *b* The temperature slightly above the conclusion temperature of the overall gelatinization endotherms.

has decreased to below room temperature (*10*). For amorphous starch gels of higher moisture content, where ice forms, $T_g{}^*$ (often called T_g in the literature) and T_g' values have been reported in a range between −3 and −10 °C for various types of starch gels (*11*−*14*). Note that this variation might partly be due to the different experimental conditions used. Both the water content and the maximum heating temperature greatly affect the extent of granule disruption during gelatinization (*15*). Starch gels obtained under different gelatinization conditions may have different structures, which may influence their glass transition behaviors. Lim et al. (*13*) reported that for potato starch heated in excess water (0.1−0.2% starch), T_g' values of the totally gelatinized samples were slightly lower than those of the partially gelatinized samples. $T_g{}^*$ and T_g' values of the gelatinized starch gels were also reported to vary with the initial water content. As the initial water content increases, $T_g{}^*$ and T_g' of fully gelatinized rice starches also increase (*11, 14*). Starches from different botanical origins, having different amylopectin crystallinity types and amylose contents, also have different gelatinization behaviors (*16, 17*). Under similar experimental gelatinization conditions, gels of starches from different botanical origins might not have the same glass transition characteristics. Unfortunately, information on this subject is still lacking.

The objective of this work is to investigate the glass transition in frozen starch gels prepared from starch with different botanical origins, subjected to a range of gelatinization conditions through varying the water contents and the heating temperatures. In this way, insights might be gained as to the changes in starch−water interactions during gelatinization. The information obtained from this study may assist in understanding the glass transitions of more complicated food products, which have gelatinized starch as a major component, such as French fries, frozen cooked rice, and noodles.

MATERIALS AND METHODS

Sample Preparation. Waxy corn, normal corn, and potato starches were purchased from Sigma-Aldrich, Inc. (St. Louis, MO). Smooth pea starch (Accu-Gel) was obtained from Parrheim Foods (Manitoba, Canada). Normal corn, potato, and pea starches, representing A, B, and C type starches, respectively, were used to determine the effects of amylopectin crystallinity pattern. The waxy corn starch was used as a pure amylopectin system. Hydrated starch samples with water contents

ranging from 1.1 to 3.0 g water/g dry starch were prepared by weighing the required amounts of starch (with approximately 10% moisture) and water into a preweighed differential scanning calorimetry (DSC) volatile sample pan. The pan was sealed, reweighed, and equilibrated overnight before the experiment. The approximate weight of the starch−water mixture in the DSC pan was 15 mg. The exact moisture content was confirmed after collecting the calorimetric data.

DSC Determination of Glass Transition in Gelatinized Starch−Water Systems. A DSC (Pyris 1, Perkin-Elmer, Norwalk, CT) with Pyris operation software was used for the determination of the glass transition temperature of the partially freeze-concentrated phase ($T_g{}^*$), heat capacity change (ΔC_p) at the glass transition region, frozen water (FW), unfrozen water (UW), and additional unfrozen water (AUW) resulting from gelatinization in starch−water systems. The calorimeter was equipped with an Intracooler 2P (Perkin-Elmer) and nitrogen gas purge. An empty volatile sample pan was used as a reference. Each starch−water mixture in a DSC pan was heated to a temperature near the peak temperature of the first gelatinization endotherm (T_1) to get partially gelatinized starch or slightly above the conclusion temperature of the overall gelatinization endotherm (T_2) to get fully gelatinized starch. T_1 and T_2 are different depending on initial water content and starch type, as listed in **Table 1**. The gelatinized sample was then cooled and rescanned from −40 °C to observe the glass transition, with or without annealing (**Figure 2a**). All measurements were done in triplicate. On completion of the experiment sequence in **Figure 2a**, the volatile sample pan was punctured and dried overnight in an oven at 115 °C and then reweighed to determine the exact water content in the sample.

$T_g{}^*$ values were reported as an onset temperature ($T_{g,onset}{}^*$) as well as a midpoint temperature ($T_{g,midpoint}{}^*$). The first value was obtained from the onset temperature in the heat flow curve while the latter value was obtained from the peak temperature of the first derivative of the heat flow curve (*18*), as illustrated in **Figure 2b**. The annealing temperatures were selected near $T_{g,onset}{}^*$ (within 1 °C difference) and slightly below $T_{g,midpoint}{}^*$ (1−3 °C lower).

ΔC_p values were calculated using the baseline difference before $T_{g,onset}{}^*$ and after the end of ice melting, with an adjustment for FW (eq 1).

$$\Delta C_p \text{ (J/g dry starch °C)} = \frac{\text{hf}_{20}{}^* - \text{hf}_{-20}{}^* \text{ (mJ/s)}}{\text{scan rate (°C/s)} \times w_{ds} \text{ (mg)}} \quad (1)$$

where w_{ds} is the weight of dry starch in the sample, $\text{hf}_{20}{}^*$ and $\text{hf}_{-20}{}^*$ are the heat flows at 20 (after the end of ice melting) and −20 °C (before $T_{g,onset}{}^*$), excluding the contribution of the heat capacity of FW. The calculation of hf* is shown in eq 2.

$$\text{hf}^* \text{ (mJ/s)} = \text{hf (mJ/s)} - \{w_{fw} \text{ (mg)} \times C_{p,water} \text{ (mJ/mg °C)} \times$$
$$\text{scan rate (°C/s)}\} \quad (2)$$

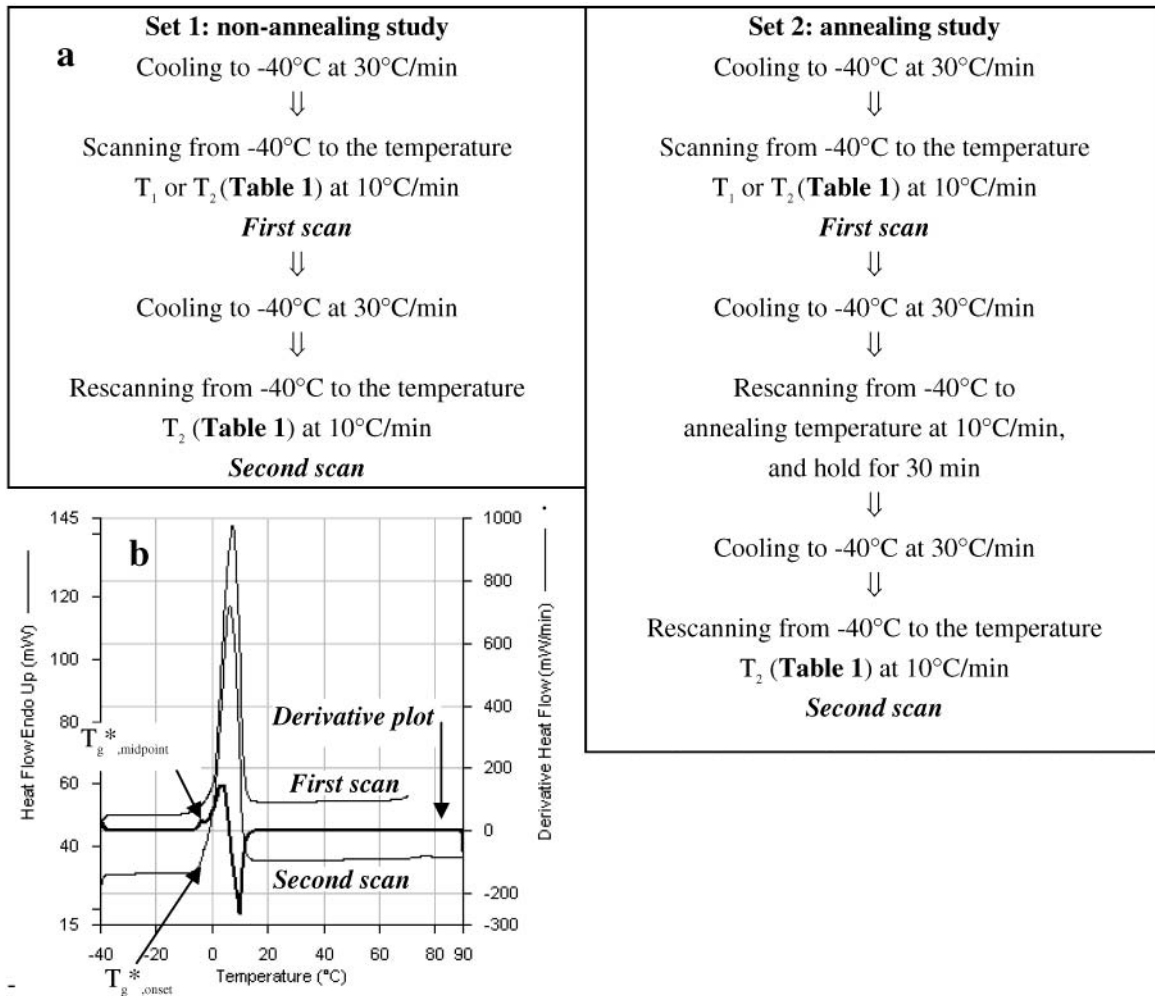where hf is the real heat flow at the corresponding temperature, $C_{p,water}$

Figure 2. Description of the experimental procedure: (**a**) flowchart for the temperature program used in the DSC study and (**b**) DSC thermograms of waxy corn starch, 3.0 g water/g dry starch, using the temperature program in set 1. The first scan was stopped at 72.5 °C (T_1, **Table 1**). The second scan was used to locate $T_{g,onset}^*$ while the first derivative plot of the second scan (shown in the thermogram) was used to locate $T_{g,midpoint}^*$.

Table 2. Amount of UW Obtained from the *x*-Axis Intercept of the Plot of FW Content vs Initial Water Content

| | amount of UW (g water/g dry starch) | | | | |
| | | nonannealed | | annealed | |
starch	ungelatinized	partially gelatinized	fully gelatinized	partially gelatinized	fully gelatinized
waxy corn	0.348 ± 0.006^a	0.375 ± 0.003	0.468 ± 0.003	0.364 ± 0.005	0.424 ± 0.009
normal corn	0.333 ± 0.010	0.354 ± 0.003	0.442 ± 0.006	0.344 ± 0.006	0.409 ± 0.003
potato	0.430 ± 0.009	0.443 ± 0.006	0.473 ± 0.004	0.422 ± 0.008	0.433 ± 0.015
pea	0.354 ± 0.011	0.391 ± 0.004	0.417 ± 0.004	0.350 ± 0.005	0.394 ± 0.005

a Represent one standard deviation from means.

is the heat capacity of water in different states, taken to be 2.1 mJ/mg °C for ice (used for the calculation of hf_{-20}^*) and 4.2 mJ/mg °C for liquid water (used for the calculation of hf_{20}^*), and w_{fw} is the weight of FW. To minimize an error from the dependence of the latent heat on temperature, w_{fw} was calculated from the difference between the initial water content (w_i) and the amount of UW (w_{uw}) obtained from the *x*-axis intercept of a plot of FW (calculated from the area under the ice melting endotherm) vs the initial water content. The calculation of w_{fw} is shown in eq 3.

$$w_{fw} \text{ (mg)} = w_{ds} \text{ (mg)} \times \{w_i \text{ (g water/g dry starch)} - w_{uw} \text{ (g water/g dry starch)}\} \quad (3)$$

w_{uw} values of various starch−water systems were shown in **Table 2**.

The calculation in eq 3 is based on the assumption that UW is not dependent on the initial water content. However, to consider the variation of UW at different initial water contents, AUW arising from the gelatinization process was calculated as the difference between FW of sequential scans in **Figure 2a**.

$$AUW_{nonanneal} = FW_{first\ scan,set1} - FW_{second\ scan,set1} \quad (4)$$

$$AUW_{anneal} = FW_{first\ scan,set2} - FW_{third\ scan,set2} \quad (5)$$

where $AUW_{nonanneal}$ and AUW_{anneal} represent the AUW (g water/g dry starch) resulting from gelatinization without and with annealing, respectively.
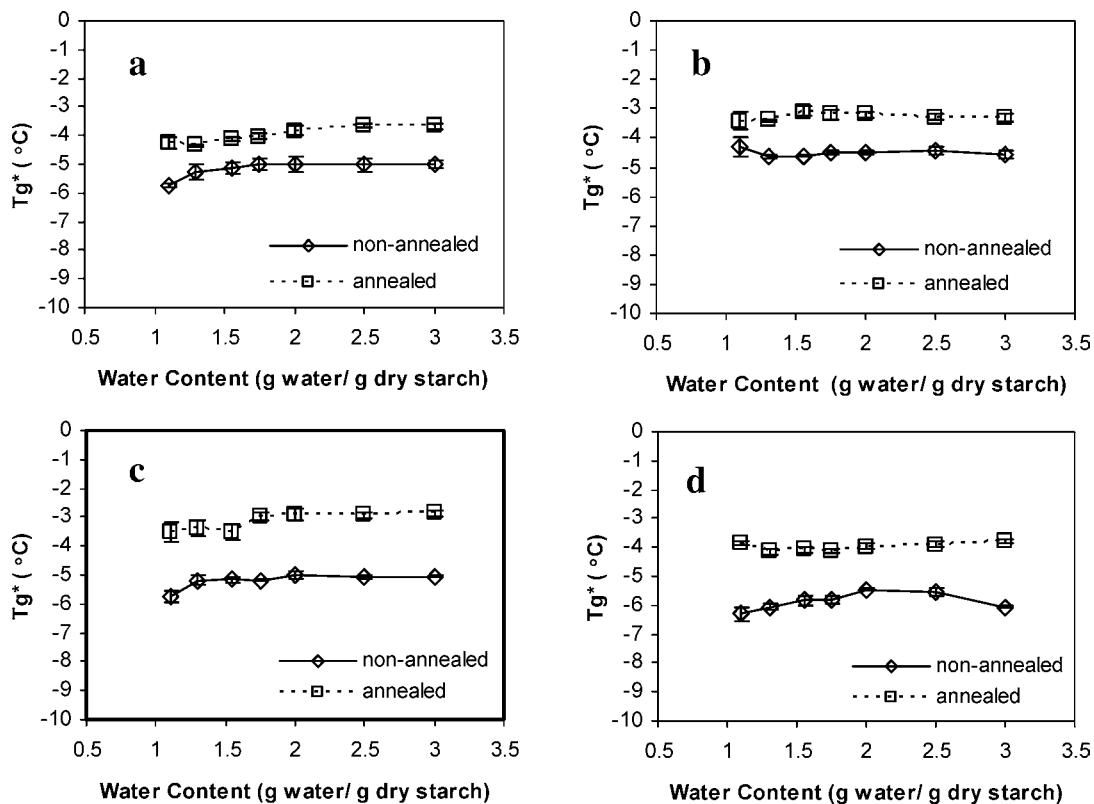
Glass Transition in Frozen Starch Gels

J. Agric. Food Chem., Vol. 52, No. 13, 2004   **4311**

Figure 3. $T_{g,onset}^{*}$ of the partially gelatinized starch gels at different water contents: (**a**) waxy corn starch, (**b**) normal corn starch, (**c**) potato starch, and (**d**) pea starch. Error bars extend one standard deviation above and below the average.
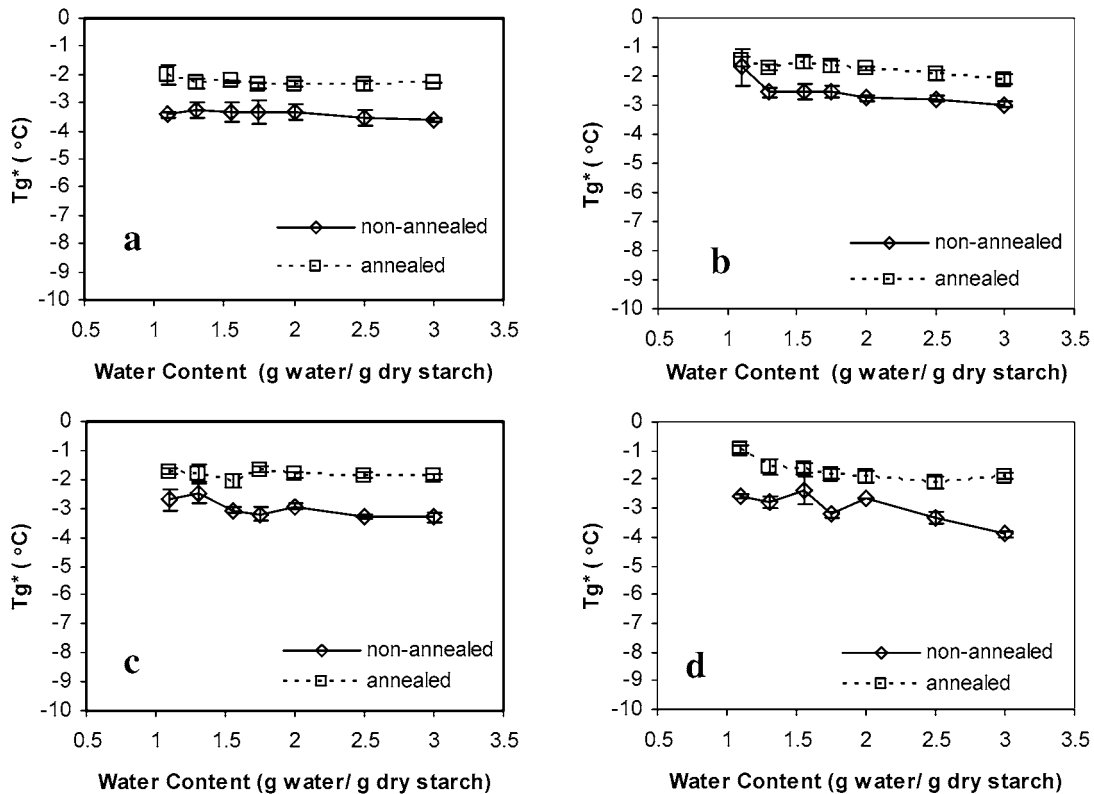

Figure 4. $T_{g,midpoint}^{*}$ of the partially gelatinized starch gels at different water contents: (**a**) waxy corn starch, (**b**) normal corn starch, (**c**) potato starch, and (**d**) pea starch. Error bars extend one standard deviation above and below the average.

RESULTS AND DISCUSSION

Effect of Water Content and Maximum Heating Temperature on Glass Transition Temperature of Gelatinized Starches. T_{g}^{*} values of various starch gels as affected by water content and maximum heating temperature are shown in **Figures 3–6**. Note that there is a slight difference between the exact initial water content and the average value, with the standard deviation up to 5% of the average water content. Because the
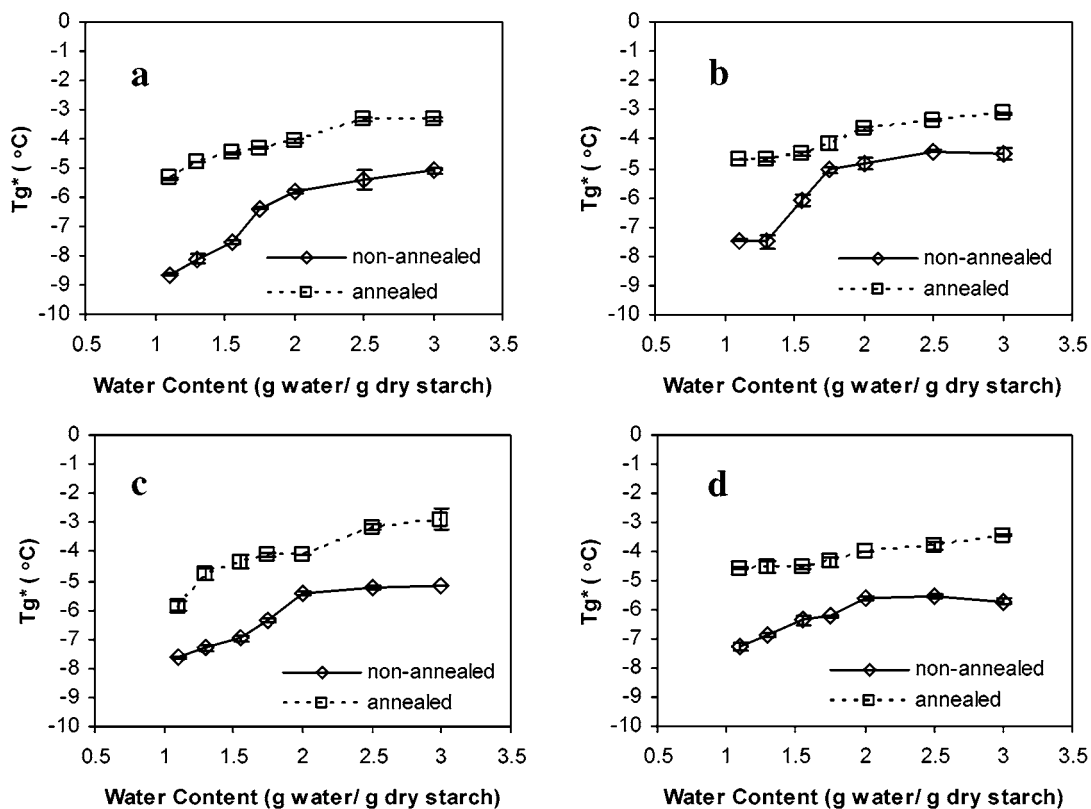
4312 *J. Agric. Food Chem.,* Vol. 52, No. 13, 2004

Tananuwong and Reid

Figure 5. $T_{g,onset}^*$ of the fully gelatinized starch gels at different water contents: (**a**) waxy corn starch, (**b**) normal corn starch, (**c**) potato starch, and (**d**) pea starch. Error bars extend one standard deviation above and below the average.
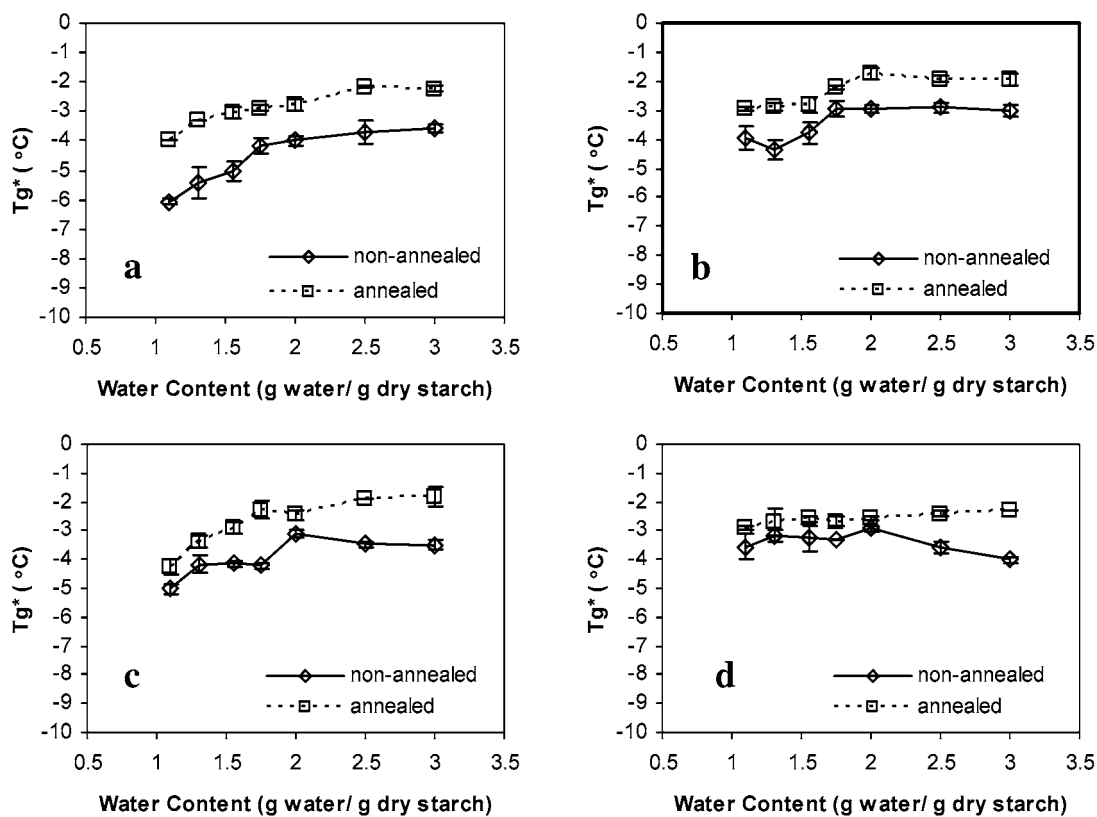

Figure 6. $T_{g,midpoint}^*$ of the fully gelatinized starch gels at different water contents: (**a**) waxy corn starch, (**b**) normal corn starch, (**c**) potato starch, and (**d**) pea starch. Error bars extend one standard deviation above and below the average.

variation of $T_{g,onset}^*$ and $T_{g,midpoint}^*$ as a function of initial water content of each starch gel is similar, both parameters will be discussed together using a general term T_g^*. For partially

gelatinized starch gels, T_g^* values are much less dependent on their initial water contents (**Figures 3** and **4**), as compared to fully gelatinized starch gels, for which the T_g^* values tend to
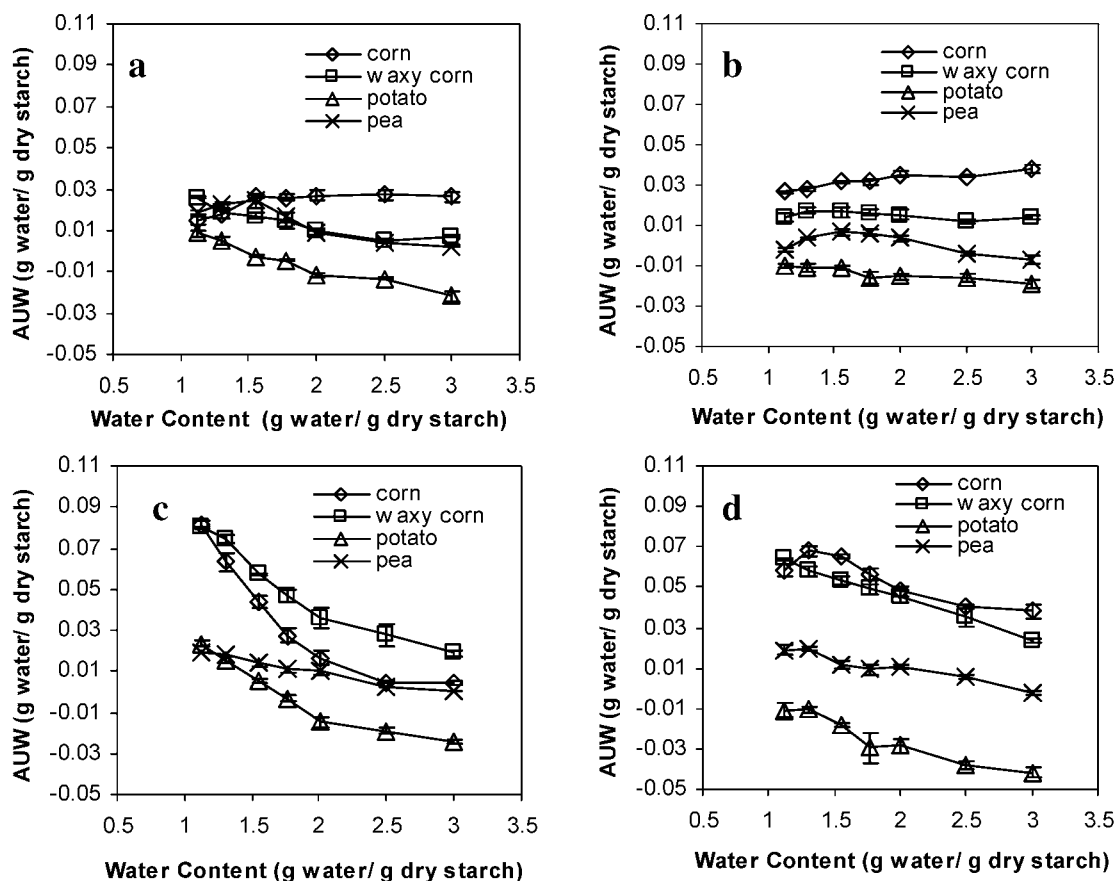
Glass Transition in Frozen Starch Gels

J. Agric. Food Chem., Vol. 52, No. 13, 2004 **4313**

Figure 7. AUW arising from gelatinization in different starch gels: (**a**) partially gelatinized, nonannealed; (**b**) partially gelatinized, annealed; (**c**) fully gelatinized, nonannealed; and (**d**) fully gelatinized, annealed. Error bars extend one standard deviation above and below the average.

increase with increasing initial water content (**Figures 5** and **6**). The increase in T_g^* and T_g' of fully gelatinized starch gels at a higher water content has been previously reported (*11*, *14*). Because a frozen starch gel is composed of an ice phase and a freeze-concentrated, unfrozen phase, the location of the glass transition of the unfrozen phase may not be simply explained as resulting from the plasticization effect of the initial water content since some of this water ends up as ice and therefore nonplasticizing. The existence of the different levels of structural disruption that result from different degrees of gelatinization, different gel structures, as well as the amount of UW in the system may also influence T_g^*. Note that a starch gel can be considered as a phase-separated system in which swollen, amylopectin-enriched granules are embedded in a continuous matrix of entangled amylose molecules (*19*). Freeze concentration results in many small, discrete ice crystals embedded in a continuous matrix of amorphous, freeze-concentrated solute (or a heterogeneous matrix of starch polymers in this case) and UW (*8*). However, to simplify the explanation, the following discussion regarding the unfrozen matrix in the gel will consider the hydrated amylose−amylopectin composite as a single phase.

The extent and nature of starch gelatinization is usually modulated by temperature and/or water content. In a DSC thermogram, two endothermic peaks have been related to the gelatinization process. These can be labeled as G (the first endotherm) and M1 (the second endotherm) (*20*). Most of the mechanisms proposed to explain these phenomena assume a solvent-assisted disruption of the starch granule structure (*15*, *20−22*). An overview of the gelatinization mechanism suggests that in excess water, starch−water interactions during the processes associated with the G endotherm are initiated within

amorphous regions and are followed by extensive disruption of the crystallites. At a decreased water content, the hydration in the amorphous regions is not sufficient to facilitate extensive crystalline disruption. The changing associations of water within the system, including increasing hydration of disentangled starch polymers, renders some water molecules less available for aiding crystalline melting. As a result, a higher thermal energy is required to enable disruption of more stable crystallites. This leads to the appearance of a separable M1 endotherm. In partially gelatinized starch gels heated only to the peak temperature of the G endotherm, a limited level of structural disruption, as evidenced by the limited crystallinity loss, would occur. For samples of intermediate water content (approximately 0.9−1.5 g water/g dry starch), wide-angle X-ray scattering studies of starch from different botanical sources have shown that a significant reduction in the crystallinity levels of starch granules occurs on attaining temperatures greater than the peak temperature of the G endotherm (*16*, *23*, *24*). Indeed, at higher water contents (above 1.5 g water/g dry starch), some (although smaller) amylopectin crystallinity can still be detected by X-ray diffraction at the peak temperature of the G endotherm (*24*). Such a limited level of structural disruption might not greatly alter the structural characteristics of starch polymers within the unfrozen phase. Thus, T_g^* of the system shows little change with increasing water content. In contrast, full gelatinization appears to result in a more extensive structural disruption, as indicated by a greater loss of amylopectin crystallinity (*16*, *23*, *24*), a higher degree of granule swelling, and polymer solubilization (*25*, *26*). A gel matrix with a more homogeneous, higher level amorphous structure as compared to that of the partial gelatinization is to be expected. Our results show that the T_g^*
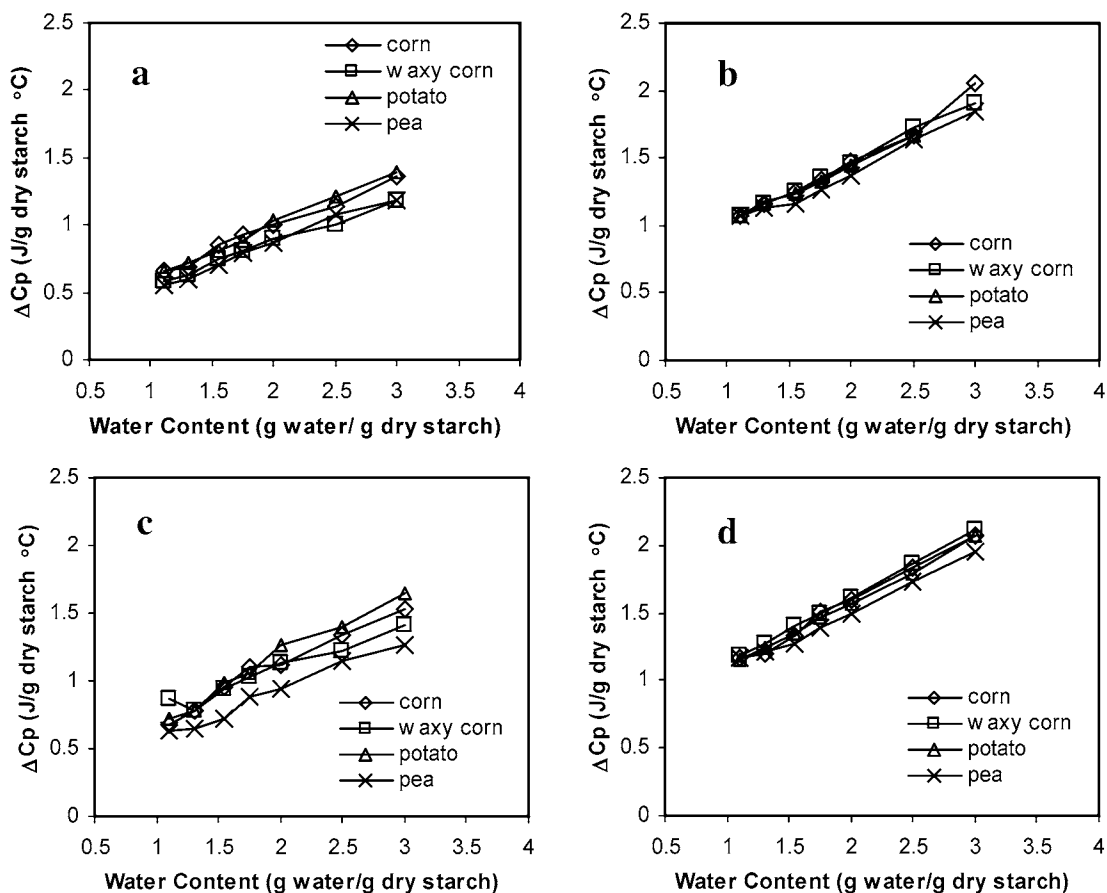
Figure 8. Change of specific heat capacity (ΔC_p) at the glass transition region in different starch gels: (**a**) partially gelatinized, nonannealed; (**b**) partially gelatinized, annealed; (**c**) fully gelatinized, nonannealed; and (**d**) fully gelatinized, annealed. Error bars extend one standard deviation above and below the average.

values of fully gelatinized starch gels with a lower moisture content, 1.1−1.5 g water/g dry starch (biphasic endotherm region, where overlapping between the G and the M1 endotherms is observed), are lower than those of the partially gelatinized gels. However, an unexpected observation is that the "dense" gel matrix, presumed to have a more concentrated polymer dispersion in the unfrozen phase, behaves rather like a more dilute glass with a lower T_g*. Perhaps there is an effect of starch−water interactions within the gel network, which greatly retards ice formation and thus slows down the rate of concentration increase of the unfrozen phase during cooling.

Starch−water interactions can be investigated by following the change in the physical state of water. One approach is to measure UW, the water within a system that does not freeze out as ice at subfreezing temperatures. UW has been proposed to be associated in some way more closely with the solute molecules although it may not be totally immobilized or "bound" (*27, 28*). Previous studies have shown that FW is linearly related to the initial water content of the system, with a regression slope close to 1 (*29*). On the basis of the assumption that UW is not dependent on the initial water content, UW values of different starch−water systems, determined from the *x*-intercept of the plot of FW against the initial water content, are listed in **Table 2**. However, the calculation of AUW shows that UW may be dependent on the initial water content (**Figure 7a,c**). This might result from differences in the gel structure. A greater extent of structural disruption after full gelatinization could expose more sugar hydroxyl groups to the solvent, resulting in increased starch−water interactions. The gel structure of more concentrated starch systems has been described as a tightly packed

aggregate of swollen granules with a thin layer of amylose gel between the granules (*25, 30*). It is proposed that this type of dense gel structure would provide a shorter distance between the water molecules and the surface of polymers and a higher area density of hydrogen bonds, which would increase the extent of the hydration (*31*). During rapid cooling in the DSC, the interactions between the water and the matrix of tangled polymers may retard the separation and spatial rearrangement of water molecules necessary to form ice. Therefore, because of kinetic constraints, a more dilute unfrozen phase may be present in the fully gelatinized gels, resulting in the observed reduction of T_g* in the system. As the total water content increases beyond that of samples which exhibit the biphasic endotherm region, T_g* of the fully gelatinized gels gradually increases and approaches that of the partially gelatinized gels (**Figures 5** and **6**). **Figure 7c** shows that the AUW of the fully gelatinized gels decreases as the water content rises, suggesting a reduced extent of starch−water interactions presumably due to a more swollen gel network. In this case, the larger distance between the polymer surfaces and larger clusters of contiguous water molecules would facilitate increased ice formation. Despite the higher initial water content, the lower observed UW of the system results in a more concentrated unfrozen matrix, leading to the observed increase of the T_g*.

Effect of Starch Types from Different Botanical Sources on Glass Transition Temperature of Gelatinized Starches. For the same maximum heating temperature, all starch types exhibit a relatively similar trend in the difference in T_g* as a function of the initial water content. However, variation in the T_g* values of the gels from different starch sources is observed.
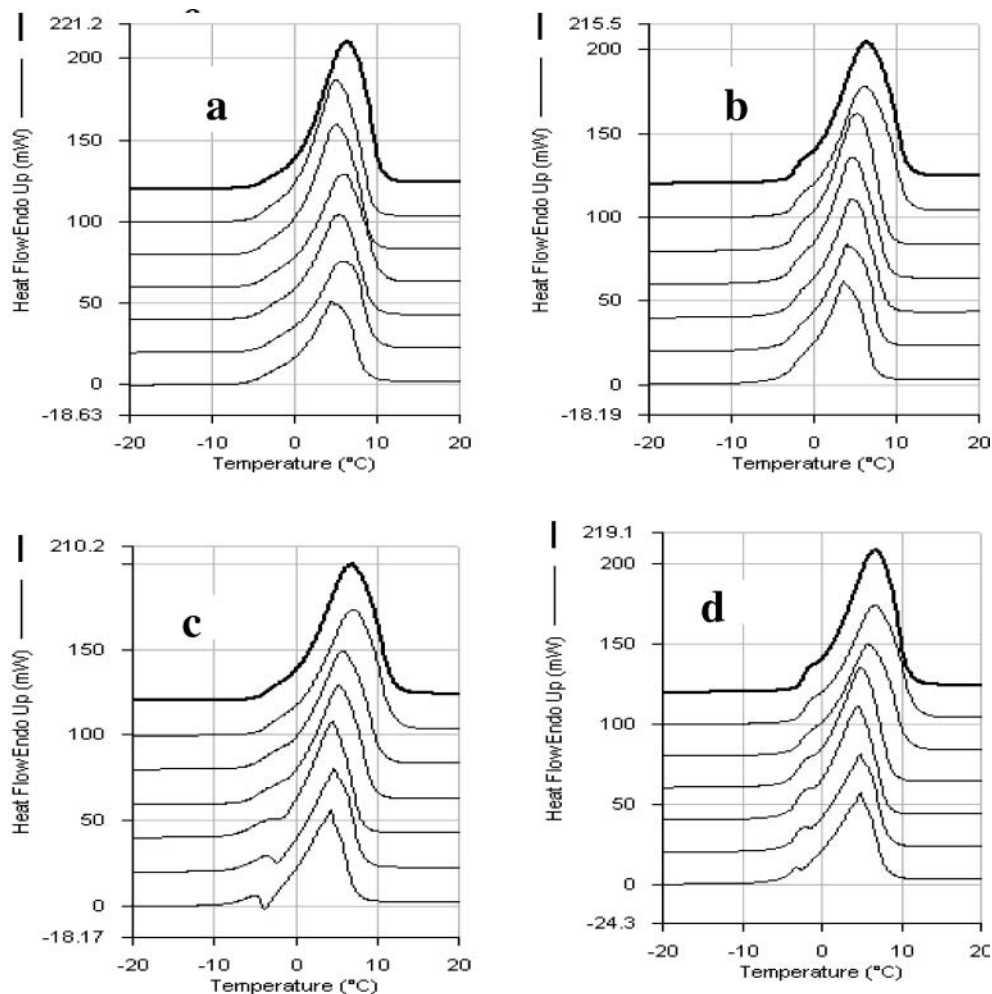
Glass Transition in Frozen Starch Gels

J. Agric. Food Chem., Vol. 52, No. 13, 2004 **4315**

Figure 9. Ice melting endotherms of waxy corn starch gels: **(a)** partially gelatinized, nonannealed; **(b)** partially gelatinized, annealed; **(c)** fully gelatinized, nonannealed; and **(d)** fully gelatinized, annealed. The water contents of the system from the upper to the lower curve are 3.0, 2.5, 2.0, 1.75, 1.5, 1.3, and 1.1 g water/g dry starch.

For nonannealed, partially gelatinized starch gels (**Figures 3** and **4**), at a similar initial water content, $T_{g,onset}*$ ranges from -6.5 to -4 °C while $T_{g,midpoint}*$ is from -4 to -1.5 °C. For nonannealed, fully gelatinized starch gels, both $T_{g,onset}*$ and $T_{g,midpoint}*$ are more dependent on the initial water content (**Figures 5** and **6**). At 1.1 g water/g dry starch, $T_{g,onset}*$ ranges from -8.6 to -7.3 °C whereas $T_{g,midpoint}*$ ranges from -6.4 to -3.6 °C. Both of the T_g* values increase with increasing initial water content to the range of -5.7 to -4.5 °C for $T_{g,onset}*$ and -4.0 to -3.0 °C for $T_{g,midpoint}*$ at 3.0 g water/g dry starch. At the same water content, the $T_{g,midpoint}*$ values of the fully gelatinized gels from normal corn and potato starches reported in this study are slightly higher than the equivalent T_g in the literature (*13, 32*). This might be due to the different temperature scanning rate and/or sample size used.

Effect of Annealing on Glass Transition Temperature of Gelatinized Starches. For a frozen system, the formation of an amorphous unfrozen matrix by freeze concentration is time-dependent. The high viscosity of an unfrozen solution at a subfreezing temperature, a reflection of restricted polymer mobility, especially at a high solute concentration, can result in a reduced rate of ice formation (*6*). Annealing at a temperature that allows for sufficient polymer mobility to enable an enhanced rate of ice formation without there being a significant reduction in the maximum possible ice content will maximize ice formation (*13*). For several carbohydrate solutions including sugars and maltodextrins, the glass transition occurs well below

the onset of ice melting and those phenomena can be separately observed (*5, 33*). Roos and Karel (*34*) recommended annealing such systems at a temperature above the estimated T_g' but slightly below T_m', the temperature of onset of equilibrium ice melting. However, the temperature difference between T_g' and T_m' decreases with increasing solute molecular weight. Hence, for high molecular weight compounds including starches, the glass transition overlaps with ice melting and their T_g' and T_m' values are predicted to be similar (*34*). In this study, we annealed the starch gels at $1-3$ °C below $T_{g,midpoint}*$. An increase in T_g* after annealing at these temperatures (**Figures 3–6**) suggests an increasing level of freeze concentration, resulting in a higher concentration of the glassy phase with an elevated T_g*. However, our arbitrary annealing time of 30 min may not be sufficient to produce the maximally freeze-concentrated phase. Verification of the dependence of the time required to maximize freeze concentration as a function of initial composition is a project in itself and was not a part of this study. After annealing, the UW of the starch gels shown in **Table 2** is lower than that of their nonannealed counterparts. The annealed samples tend to have lower AUW especially for lower initial water contents in the cases of both partially and fully gelatinized starch gels (**Figure 7**). These results suggest that additional water migrates to form ice during the annealing process, leaving a reduced amount of UW within the systems. Thus, the changes in UW

and AUW support our presumption of an increase in freeze concentration associated with the annealing conditions used in this study.

Changes in Specific Heat Capacity during Glass Transition in Frozen Starch Gels. Figure 8 depicts the effects of various factors on the magnitude of ΔC_p during the glass transition in different starch gels. Without annealing, although ΔC_p values are slightly higher in the fully gelatinized gels, a similar trend of the change in ΔC_p as a function of initial water content is found for both partially and fully gelatinized gels (**Figure 8a,c**). The observed increase in ΔC_p might result from a formation of a larger amount of amorphous glassy matrix (*13*) and/or the occurrence of a greater extent of structural disruption, which might result in a reduced molecular weight of starch polymers due to a greater degree of amylopectin disentanglement and concomitant fragmentation. Because, for several carbohydrate solutions, Roos and Karel (*34*) reported an increase in ΔC_p (J/g solids °C) over the glass transition region as the molecular weight of the solute decreases, the potential reduction in average polymer molecular weight might partly account for the ΔC_p increase. After annealing, ΔC_p further increases (**Figure 8b,d**) possibly due to structural relaxations. Annealing at sub-T_g or near T_g allows the system to approach metastable equilibrium with some extra loss in enthalpy and volume (*4*). When the structural relaxation takes place near the glass transition temperature, an enthalpy overshoot at T_g is often observed (*35*). However, the enthalpy overshoot is not easily detected in the annealed starch gels (**Figure 9b,c**), probably due to the overlap between the glass transition and the ice melting, and to the low level of structural relaxation expected within the short annealing time used in this study (30 min). All types of starch used in this study show a similar trend in the variation of ΔC_p as a function of water content.

Devitrification in Frozen Starch Gels. In frozen aqueous biopolymer systems, various transitions have been identified during rewarming of rapidly cooled systems. A glass transition is usually detected first, followed by devitrification or ice formation, characterized by an exotherm in the DSC thermogram, which occurs immediately after the glass transition (*5, 6, 18, 36*). Devitrification may result from the increasing mobility of starch polymers in the matrix, reflected in the decreasing viscosity of the rubbery unfrozen matrix, which eliminates some physical constraints for the ice formation (*6, 14*). For frozen starch gels, our results clearly show a devitrification exotherm in some fully gelatinized systems of lower water content (**Figure 9c**). This can be observed in the gels from waxy corn, normal corn, and potato starches but not from pea starch, which does not exhibit the devitrification exotherm under any treatment conditions (data not shown). During rewarming of the frozen fully gelatinized starch gels, the magnitude of the exotherm decreases as the water content increases, with no exotherm observed above 1.75 g water/g dry starch for waxy corn, 1.5 g water/g dry starch for potato, and 1.3 g water/g dry starch for native corn starch gels. This trend corresponds to previous studies in rice starch gels (*11*) and in fructose and glucose solutions (*37*). The larger extent of ice formation during the rewarming process in gels with lower water content may be due to the larger AUW in these systems (**Figure 7c**). In contrast, no devitrification exotherm is seen in partially gelatinized gels from all of the types of starch used (**Figure 9a,b**). This may be related to the relatively lower amount of AUW in the partially freeze-concentrated phase (**Figure 7a**). Annealing also influences the devitrification process. As discussed earlier, annealing enhances ice formation and thus

decreases UW in the systems. Therefore, it greatly decreases the magnitude of the exotherm (**Figure 9d**). It is important to note that by considering systems that may exhibit devitrification exotherms, we are mainly interested in the kinetically defined "real" state diagram instead of the theoretical state diagram (**Figure 1**).

LITERATURE CITED

(1) Slade, L.; Levine, H. Water relationships in starch transitions. *Carbohydr. Polym.* **1993**, *21*, 105−131.

(2) Jouppila, K.; Roos, Y. The physical state of amorphous corn starch and its impact on crystallization. *Carbohydr. Polym.* **1997**, *32*, 95−104.

(3) Roos, Y. H.; Karel, M.; Kokini, J. L. Glass transitions in low moisture and frozen foods. *Food Technol.* **1996**, *11*, 95−108.

(4) Le Meste, M.; Champion, D.; Roudaut, G.; Blond, G.; Simatos, D. Glass transition and food technology, a critical appraisal. *J. Food Sci.* **2002**, *67*, 2444−2458.

(5) Levine, H.; Slade, L. A polymer physicochemical approach to the study of commercial starch hydrolysis products (SHPs). *Carbohydr. Polym.* **1986**, *6*, 213−244.

(6) Roos, Y.; Karel, M. Amorphous state and delayed ice formation in sucrose solutions. *Int. J. Food Sci. Technol.* **1991a**, *26*, 553−566.

(7) Franks, F. The properties of aqueous solutions at sub-zero temperatures. In *Water: A Comprehensive Treatise*; Franks, F., Ed.; Plenum Press: New York, 1982; Vol. 7, pp 215−338.

(8) Levine, H.; Slade, L. Principles of "cryostabilization" technology from structure/property relationships of carbohydrate/water systems—a review. *Cryo-Lett.* **1988**, *9*, 21−63.

(9) Champion, D.; Blond, G.; Simatos, D. Reaction rates at subzero temperatures in frozen sucrose solutions: a diffusion-controlled reaction. *Cryo-Lett.* **1997**, *18*, 251−260.

(10) Zeleznak, K. J.; Hoseney, R. C. The glass transition in starch. *Cereal Chem.* **1987**, *64*, 121−124.

(11) Huang, R. M.; Chang, W. H.; Chang, Y. H.; Lii, C. Y. Phase-transitions of rice starch and flour gels. *Cereal Chem.* **1994**, *71*, 202−207.

(12) Chatakanonda, P.; Varavinit, S.; Chinachoti, P. Relationship of gelatinization and recrystallization of cross-linked rice to glass transition temperature. *Cereal Chem.* **2000**, *77*, 315−319.

(13) Lim, M. H.; Wu, H. B.; Reid, D. S. The effect of starch gelatinization and solute concentrations on T_g' of starch model system. *J. Sci. Food Agric.* **2000**, *80*, 1757−1762.

(14) Chung, H. J.; Lee, E. J.; Lim, S. T. Comparison in glass transition and enthalpy relaxation between native and gelatinized rice starches. *Carbohydr. Polym.* **2002**, *48*, 287−298.

(15) Jenkins, P. J.; Donald, A. M. Gelatinisation of starch—a combined SAXS/WAXS/DSC and SANS study. *Carbohydr. Res.* **1998**, *308*, 133−147.

(16) Yuryev, V. P.; Kalistratova, E. N.; van Soest, J. G. J.; Niemann, C. Thermodynamic properties of barley starches with different amylose content. *Starch* **1998**, *50*, 463−466.

(17) Ablett, S.; Izzard, M. J.; Lillford, P. J. Differential scanning calorimetric study of frozen sucrose and glycerol solutions. *J. Chem. Soc., Faraday Trans.* **1992**, *88*, 789−794.

(18) Ring, S. G. Some studies on starch gelation. *Starch* **1985**, *37*, 80−83.

(19) Donovan, J. W. Phase transition of the starch-water system. *Biopolymers* **1979**, *18*, 263−275.

(20) Evans, I. D.; Haisman, D. R. The effect of solutes on the gelatinization temperature range of potato starch. *Starch* **1982**, *34*, 224−231.

(21) Slade, L.; Levine, H. Nonequilibrium melting of native granular starch: Part I. Temperature location of the glass transition associated with gelatinization of A-type cereal starches. *Carbohydr. Polym.* **1988**, *8*, 183−208.

Glass Transition in Frozen Starch Gels

J. Agric. Food Chem., Vol. 52, No. 13, 2004 **4317**

(22) Waigh, T. A.; Gidley, M. J.; Komanshek, B. U.; Donald, A. M. The phase transformations in starch during gelatinisation: a liquid crystalline approach. *Carbohydr. Res.* **2000**, *328*, 165−176.

(23) Svensson, E.; Eliasson, A. C. Crystalline changes in native wheat and potato starches at intermediate water levels during gelatinization. *Carbohydr. Polym.* **1995**, *26*, 171−176.

(24) Le Bail, P.; Bizot, H.; Ollivon, M.; Keller, G.; Bourgaux, C.; Buléon, A. Monitoring the crystallization of amylose-lipid complexes during maize starch melting by synchrotron X-ray diffraction. *Biopolymers* **1999**, *50*, 99−110.

(25) Garcia, V.; Colonna, P.; Bouchet, B.; Gallant, D. J. Structural changes of cassava starch granules after heating at intermediate water contents. *Starch* **1997**, *49*, 171−179.

(26) Atkin, N. J.; Abeysekera, R. M.; Cheng, S. L.; Robards, A. W. An experimentally based predictive model for the separation of amylopectin subunits during starch gelatinization. *Carbohydr. Polym.* **1998**, *36*, 173−192.

(27) Franks, F. Unfrozen water: yes; unfreezable water: hardly; bound water: certainly not. *Cryo-Lett.* **1986**, *7*, 207.

(28) Li, S.; Dickinson, L. C.; Chinachoti, P. Mobility of "unfreezable" and "freezable" water in waxy corn starch by ^{2}H and ^{1}H NMR. *J. Agric. Food Chem.* **1998**, *46*, 62−71.

(29) Wootton, M.; Bamunuarachchi, A. Water binding capacity of commercial produced native and modified starches. *Starch* **1978**, *30*, 306−309.

(30) Keetels, C. J. A. M.; van Vliet, T.; Walstra, P. Gelation and retrogradation of concentrated starch systems: 3. Effect of concentration and heating temperature. *Food Hydrocolloids* **1996**, *10*, 363−368.

(31) Wolfe, J.; Bryant, G.; Koster, K. L. What is "unfreezable water", how unfreezable is it and how much is there? *Cryo-Lett.* **2002**, *23*, 157−166.

(32) Ferrero, C.; Martino, M. N.; Zaritzky, N. E. Effect of hydrocolloids on starch thermal transitions, as measured by DSC. *J. Therm. Anal.* **1996**, *47*, 1247−1266.

(33) Roos, Y. Melting and glass transitions of low molecular weight carbohydrates. *Carbohydr. Res.* **1993**, *238*, 39−48.

(34) Roos, Y.; Karel, M. Water and molecular weight effects on glass transitions in amorphous carbohydrates and carbohydrate solutions. *J. Food Sci.* **1991b**, *56*, 1676−1681.

(35) Barens, A. R.; Hodge, I. A. Effects of annealing and prior history on enthalpy relaxation in glassy polymers. 1. Experimental study on poly(vinyl chloride). *Macromolecules* **1982**, *15*, 756−762.

(36) Liu, H.; Lelievre, J. Transitions in frozen gelatinized-starch systems studied by differential scanning calorimetry. *Carbohydr. Polym.* **1992**, *19*, 179−183.

(37) Roos, Y.; Karel, M. Nonequilibrium ice formation in carbohydrate solutions. *Cryo-Lett.* **1991c**, *12*, 367−376.